Academic Journal of Chemistry
ISSN(e): 2519-7045, ISSN(p): 2521-0211
Vol. 6, Issue. 2, pp: 45-59, 2021
URL: https://arpgweb.com/journal/journal/20
DOI: https://doi.org/10.32861/ajc.62.45.59

Academic Research Publishing Group

Original Research **Open Access**

Synthesis and Characterization of Novel Θ-Type Zirconium Phosphate-Crystalline Cerium Phosphate/ Polyaniline, Polyindole, Polycarbazole, Polyaniline-co-Polyindole, and Polyaniline-co-Polycarbazole Composites

S. K. Shakshooki (Corresponding Author)
Department of Chemistry, Faculty of Science University of Tripoli, Tripoli, Libya
Email: shakshooki2002@yahoo.com

F. A. El-Akari
Department of Chemistry, Faculty of Science University of Tripoli, Tripoli, Libya

Najat A. Abozaid
Department of Chemistry, Faculty of Science University of Tripoli, Tripoli, Libya

Article History
Received: 27 February, 2021
Revised: 21 April, 2021
Accepted: 22 May, 2021
Published: 26 May, 2021

Abstract

Θ-Type zirconium phosphate, Θ-$Zr(HPO_4)2$-.$1.77H_2O$ (Θ-ZrP), crystalline cerium phosphate, $Ce(HPO_4)_2$.1.33 H_2O (CePc), and $[Θ\text{-}Zr(HPO_4)_2]_{0.30}$ $[Ce\ (HPO_4)_2]_{0.70}$.$2H_2O$ composite were prepared and characterized by chemical, XRD, TGA, FT-IR and scanning electron microscopy(SEM). $[Θ\text{-}Zr(HPO_4)_2]_{0.30}[Ce(HPO_4)_2]_{0.70}$/polyaniline, polyindole, polycarbazole, polyaniline-co-polyindole, polyaniline-co-polycarbazole composites were prepared via in-situ chemical oxidation of the monomers aniline , indole , carbazole and (1:1moler ratio) of co-monomers aniline-indole, aniline-carbazole, respectively, that was promoted by the reduction of part of Ce(IV) ions present in the inorganic matrix. A possible explanation is part of CePc is attacked by the monomers, and the co-monomers, respectively, converted to cerium (III) orthophosphate ($CePO_4$). The resultant novel composites were characterized by elemental (C,H,N) analysis, FT-IR, and (SEM). From elemental (C,H,N) analysis ,the amount of organic materials present in $[Θ\text{-}Zr(HPO_4)_2]_{0.30}$ $[Ce\ (HPO_4)_2]_{0.70}$/ polyaniline, polyindole, polycarbazole composites were (23.44, 5.24 and 33.02 % in wt.), respectively. The amount of resultant copolymers were (Pani 5.92, PIn 7.48 % in wt) and (Pani 1.42, PCz 2.48 % in wt) These composites can be considered as novel conducting inorganic-organic composites, ion exchangers , solid acid catalysts and sensors.

Keywords: Θ-type zirconium phosphate; Crystalline cerium phosphate; Polyaniline; Polyindole; Polycarbazole and their copolymers composites.

1. Introduction

Tetravalent metal phosphates are very insoluble compounds with good thermal stabilities and high ion exchange capacities [1, 2]. The discovery of their crystalline materials [3, 4], represent a fundamental step in chemistry of these compounds with general formula α-$M(IV)(HPO_4)_2.H_2O$, and γ-$M(IV)PO_4.H_2PO_4.2H_2O$, (where M = Ti, Zr, Hf, Ge, Sn and Ce). These materials contain structural POH groups with labile protons. They can exchange their protons with counter ions such as alkali, alkaline earth, transition divalent and trivalent metal ions [1-4] and act as intercalates [1, 2, 5, 6]. Increase attention direct toward their intercalation [5, 6], catalytic [7], electrical conductance [8], and sensors [9]. Layered zirconium phosphates have potential applications as inorganic fillers, sorbents and solid acid catalysts [7, 10-16].

Crystalline cerium phosphates have been studied as ion exchangers, intercalates and as proton conductance. Their composition, structure and the degree of crystallinity results from reaction of solutions containing a Ce^{IV} salt is mixed with a solution of phosphoric acid of [$(PO_4)/Ce^{IV}$ ratio] [17-19], strongly dependent on the experimental conditions such as rate and order of mixing of the solutions, stirring, temperature and digestion time [20-22].

Composite materials have been the target of growing interest owing to their unique optical, electrical, mechanical, thermal, and magnetic properties arising from the combination of the different constituents on a nanometric scale. In recent years, several organic–inorganic nanocomposites have been prepared by combining organic polymers and inorganic materials, employing different methods. In some cases, a polymer is introduced into the free spaces of the inorganic compound interlayer spaces in layered solids [23-26].

Introduction of monomer molecules and their further polymerization in confined environments can also be performed [23-26]. Another approach involves the coating of core-like particles of inorganic oxides, glass fibbers, etc. This can be achieved either by adsorption of polymers on the particles or by adsorption of monomers in the cores, followed by polymerization [27-30].

Conducting polymers are a novel class of synthetic metals , called materials of 21^{st} Century , that combine the chemical, electrochemical and mechanical properties of polymers with the electronic properties of metals and

semiconductor, generated tremendous interest due to their potential applications in various fields such as rechargeable batteries, electrochromic display devices, separation membrane sensors and anticorrosive coatings on metals [23, 25, 27, 29, 31-36]. Their methods of preparation were carried out mainly by chemical oxidation polymerization and electrochemical polymerization [37-39].

The biggest advantage of conducting polymers is their process ability, low cost, and thermal stability [37, 38]. They have alternating single and double bonds in their conjugated molecules. On doping these conjugated polymers show very high conductivity similar to metal.

Conducting polymers containing nitrogen atoms such as polyaniline, polypyrrole, and polyindole and their substituted derivatives, belonging to the fused-ring family, have received increasing attention in various fields due to their unique physical, electrical and chemical properties [23, 25-27, 31-34, 36]. These materials have an important influence on electrochromic device, sensors, catalysis, anticorrosion. Their electrical and electrochemical proper-ties, owns advantages fairly good thermal stability show great promise for commercial applications [37-42]. Among conductive polymers, polyaniline and polypyrrole have attracted considerable attention, widely studied, because of their ease of preparation, low cost of monomer, good environmental stability, good conductivity control through doping as well as a good control of oxidation level. All these properties gives polyaniline and polypyrrole the potential for wide applications [41-45]. It can effectively be used as optoelectronic sensors [46-49], conductive paints and adhesives [50-52]. Polyaniline and polypyrrole have also good power and energy density [53-57].

Polyindole is an electroactive polymer, owns advantages especially fairly good thermal stability [40, 58-61]. Some studies shows polyindole has similar properties like polyaniline, based on their high conductance and good environmental stability [40, 58, 59].

Polycarbazole, although less studied among the conductive polymers, has many advantages such as cheap, environmental and chemically stable because of aromatic structure with nitrogen atom in structure. It has unique electrical, electrochemical and optical properties [62-64]. Novel nanocomposites of polybenzimidazole, polyaniline and their copolymers polypyrrole, polyindole have been reported recently [65, 66].

2. Materials and Methods

2.1. Chemicals

($ZrOCl_2.8H_2O$), H_3PO_4 (85%), of BDH, cerium sulfate, $(Ce(SO_4)_2.4H_2O)$ of Merck, aniline (99.5%) of Mindex UK, indole, carbazole and HF(40%) of Reidel de-Haen. Other reagents used were of analytical grade.

2.2. Instruments Used for Analysis

- X-ray powder diffractometry. Siemens D-500, using Ni-filtered CuK_a(λ=1.54056A$^{\circ}$) XRD with CuK_a radiation at 1.540Å by using PHILIPS PW1710.
- . TG/DTA SIIExtra6000,
- Scanning electron microscopy (SEM) Jeol SMJ Sm 5610 LV.
- Fourier Transform infrared spectrometer FT-IR, FT-IR-6100 and Shimadzu FT-IR Spectrometer in the rang 200-4000cm^{-1}.
- Carbon Hydrogen Nitrogen (CHN) automatic analyzer Varian EL III-Elemental, Germany.
- pH Meter WGW 521.

2.3. Preparation of Θ-Type Zirconium Phosphate

50ml 0.5M $ZrOCl_2.8H_2O$ in 3M HF were mixed with 200ml of (4.6M) H_3PO_4 in Pyrex round bottom flask (prior to mixing, the solutions were cooled at ~15ºC),. The mixture left at ~15ºC for 3days. The resultant precipitate was washed with distilled water, by addition and decantation of distilled water, up to pH3.The resultant product was filtered and left to dry in air.

2.4. Preparation of Crystalline Cerium Phosphate

100g of $CeSO_4.4H_2O$ were dissolved in 400ml of 10M H_3PO_4 under stirring at 80^{o}C in a glass round bottom flask. The product starts to form after few hours of stirring at that temperature, and left to digest for 4daysat 80^{o}C. The resultant precipitate was subjected to washing by distilled water up to pH=3.5, filtered and air dried to obtain crystalline cerium phosphate.

2.5. Preparation of Θ-Type Zirconium Phosphate- Crystalline Cerium Phosphate Composite (Θ-ZrP-CeP_c)

0.1g of Θ-ZrP was mixed with 0.25g of CePc in10ml ethanol, with stirring for 15 minutes at room temperature. The resultant product was filtered, washed with ethanol and left to dry in air.

2.6. Polymerization of Aniline, Indole, and Carbazole by Θ-Type Zirconium Phosphate-Crystalline Cerium Phosphate Composite

2.6.1. Preparation of Θ-Type Zirconium Phosphate-Crystalline Cerium Phosphate/Polyaniline Composite, (Θ-ZrP-CeP_c/Pani)

0.1g of Θ-ZrP was mixed with 0.25g of CeP_c in 10ml of ethanol with stirring for 15 minutes at room temperature, to that 13ml 4% aniline in ethanol was added with stirring for 48hr at room temperature. The resultant product was filtered, washed with ethanol and left to dry in air. The colour of the resultant product was bluish-green**.**

2.6.2. Preparation of Θ-Type Zirconium Phosphate-Crystalline Cerium Phosphate/Polyindole Composite, (Θ-ZrP-CeP_c/PIn)

0.1g of Θ-ZrP was mixed with 0.25g of CeP_c in 10ml ethanol with stirring for 15 minutes at room temperature, to that 16.5ml 4% indole in ethanol was added with stirring for 48hr at room temperature. The resultant product was filtered, washed with ethanol and left to dry in air. The colour of the resulting product was brownish-green**.**

2.6.3. Preparation of Θ-Type Zirconium Phosphate-Crystalline Cerium Phosphate/Polycarbazole Composite, (Θ-ZrP-CeP_c/PCz)

0.1g of Θ-Type ZrP was mixed with 0.25g of CeP_c in 10ml of ethanol with stirring for 15 minutes at room temperature, to that 23ml 4% carbazole in acetone solution were added with stirring for 48hr at room temperature. The resultant product was filtered, washed with acetone and left to dry in air. The colour of the resultant product was green**.**

2.7. Polymerization of Aniline-co-Indole and Aniline-co-Carbazole by Θ-Type Zirconium Phosphate-Crystalline Cerium Phosphate Composite

2.7.1. Preparation of Θ-Type Zirconium Phosphate Crystalline Cerium Phosphate / Polyaniline-co-Polyindole Composite, (Θ-ZrP-CeP_c/Pani-co-PIn)

A mixture of 0.1g of Θ-Type ZrP and 0.25g of CeP_c was dispersed in 10ml ethanol with stirring for 15 minutes, to that mixture of 6.5 ml 4% aniline in ethanol and 8.5ml 4% indole in ethanol was added. The stirring was continued for 48hr at room temperature (20^oC). The resultant product was filtered, washed with ethanol and left to dry in air. The colour of the product was bluish-green.

2.7.2. Preparation of Θ-Type Zirconium Phosphate - Crystalline Cerium Phosphate/Polyaniline-co-Polycarbazole Composite, (Θ-ZrP-CeP_c/Pani-co-PCz)

A mixture of 0.1g of Θ-Type ZrP and 0.25g of CeP_c was dispersed in 10ml ethanol with stirring for 15 minutes, to that mixture of 6.5 ml 4% aniline in ethanol and 11.5ml 4% carbazole in acetone was added. The stirring was continued for 48hr at room temperature (20^oC). The resultant product was filtered, washed with ethanol and acetone, then left to dry in air. The colour of the product was bluish-green.

3. Results and Discussion

Different composition structures of crystalline zirconium phosphate and cerium phosphates, $Zr(HPO_4)_2.nH_2O$, $Ce(HPO_4)_2.nH_2O$, where n=1-5 and 1-3, respectively, results from reaction of solutions containing a Zr^{IV} and Ce^{IV} salts with phosphoric acid, found to be strongly dependent on the experimental conditions. In previous studies we have found that when nanofibrous cerium phosphate membrane, $Ce(HPO_4)_2.2.9H_2O$, reacts with aniline the resultant product was polyaniline nanocomposite membrane , of black color, non-conductance [67]. However , when dilute HCl solution was added during the process of polymerization, the resultant product was Emiraldine salt nanocomposite, green color. Nanofibrous cerium phosphate act as self-support polymerization of aniline while dilute HCl act as doping agent [67]. From that we plan to arrange facile synthesis of conducting polymers cerium phosphate composites using self-support doping agent combined with cerium phosphate. Zirconium phosphates contains labile proton (H^+) present in its (POH) groups found to be the best choice for self doping.

Θ-Type zirconium phosphate, Θ-$Zr(HPO_4)_2.1.77H_2O$, was prepared from reaction of tetravalent zirconium salt, $ZrOCl_2.8H_2O$ and H_3PO_4 in HF solution. The resultant product was characterized by chemical, XRD, thermal analysis and by FT-IR spectroscopy. Its exchange capacity was determined by Na^+ ions titration.

3.1. XRD of Θ-ZrP

Figure 1 shows the X-ray powder diffraction pattern of the Θ-type zirconium phosphate, with presence of diffraction maxima, basal spacing equal 9.85Å. The Θ-type material exhibit lamellar structure. Negatively charged layers are formed by macro anions $[M(IV)(HPO_4)_2]^{-2n}$ and protons (H^+) bonded to the oxygen adjacent to the anionic layer form positively charged layers. The water molecules occupying crystallographic sites are located almost in the center of interlayer cavities.

Figure-1. X-ray diffractogram of Θ-ZrP

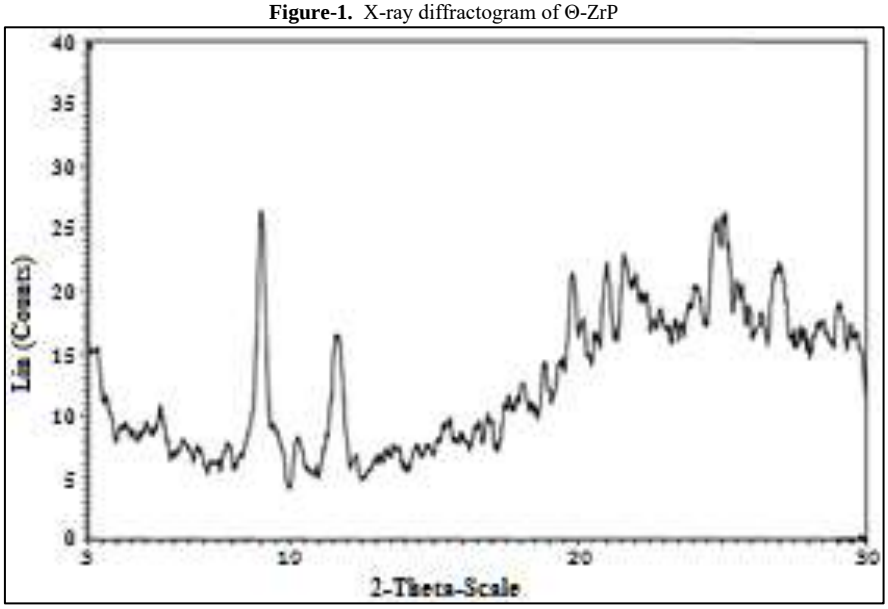

3.2. FT-IR of Θ-ZrP

Figure 2 shows FT-IR spectrum of Θ-type zirconium phosphate in the range 4000-400cm^{-1} wave number. The narrow bands at 3604.65, 3434.11cm^{-1} are assigned to vibration modes of H_2O molecules, suggest that water molecules are located at well defined crystallographic sites. These bands at 3434.11, 3434.11cm^{-1} were also attributed to O-H asymmetric modes of interlayer water molecules. The band at 1640cm^{-1} corresponds to H-O-H bending modes. The broad band at 3147.10cm^{-1} assigned to (POH) stretching mode of the hydrogen bond, it had shoulder at 3310cm^{-1} attributed to O-H stretching coming from symmetry lowering effect of the H_2O interlayer molecules. The bands at the region 1273.21-1054.46cm^{-1} are assigned as P-O asymmetry stretching of PO_4 groups, while a band at 976.33cm^{-1} is characteristic to the bonding in plane of the (P-O) bond. The bands in the region 609.14 to 515.39cm^{-1} ascribed to the presence of δ(PO_4) and to vibration of water molecules , while the band at 671.64cm^{-1} is connected with O-H bond (out of plane). A tentative assignment of various vibration modes is proposed based on previous works preformed in other M(IV) phosphate compounds [1, 2].

Figure-2. FT-IR spectrum of Θ-ZrP

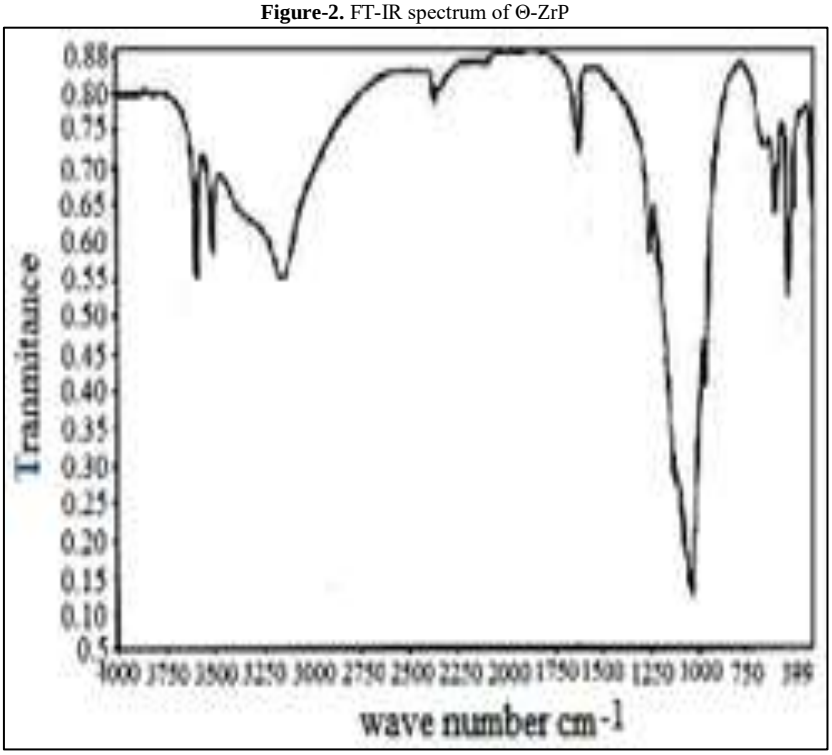

3.3. TG/DTA of Θ-ZrP

Thermal analysis of Θ-type Zr(HPO4)2.1.77H2O is shown in Figure 3, was carried out at temperature range 25-800℃ in air atmosphere. The heating rate was 10ºC/min. The thermal decomposition exhibits two weight loss stages, the loss of water of hydration followed by POH groups condensation. The final product was ZrP_2O_7. The thermal decomposition found to follow the same trends of thermal decomposition of tetravalent metal phosphates [1-3]. The thermal decomposing was accompanied by endothermic peaks.

Figure-3. TG/DTA of Θ-ZrP

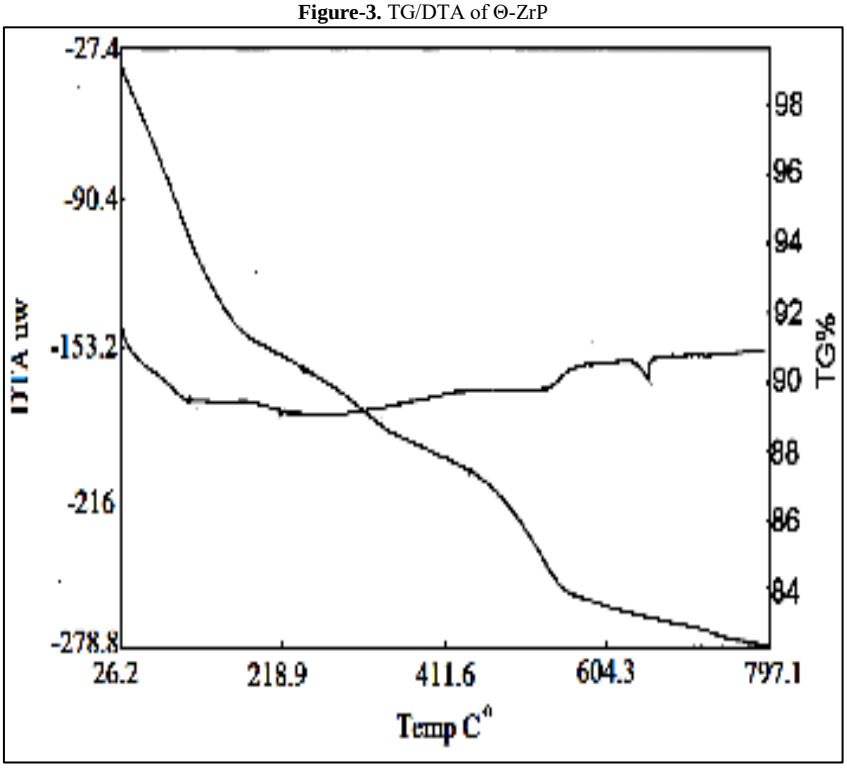

3.4. Exchange Capacity of Θ-ZrP

Exchange capacity of Θ-type zirconium phosphate was determined by Na^+ ions titration. The titration curve is shown in Figure 4. The exchange capacity found to be equal to 6.2Meq/g. The calculated value is 6.01Meq/g. The difference is due to partial hydrolysis of HPO_4 groups due to pH effect.

Figure-4. Na^+ titration curve of Θ-ZrP

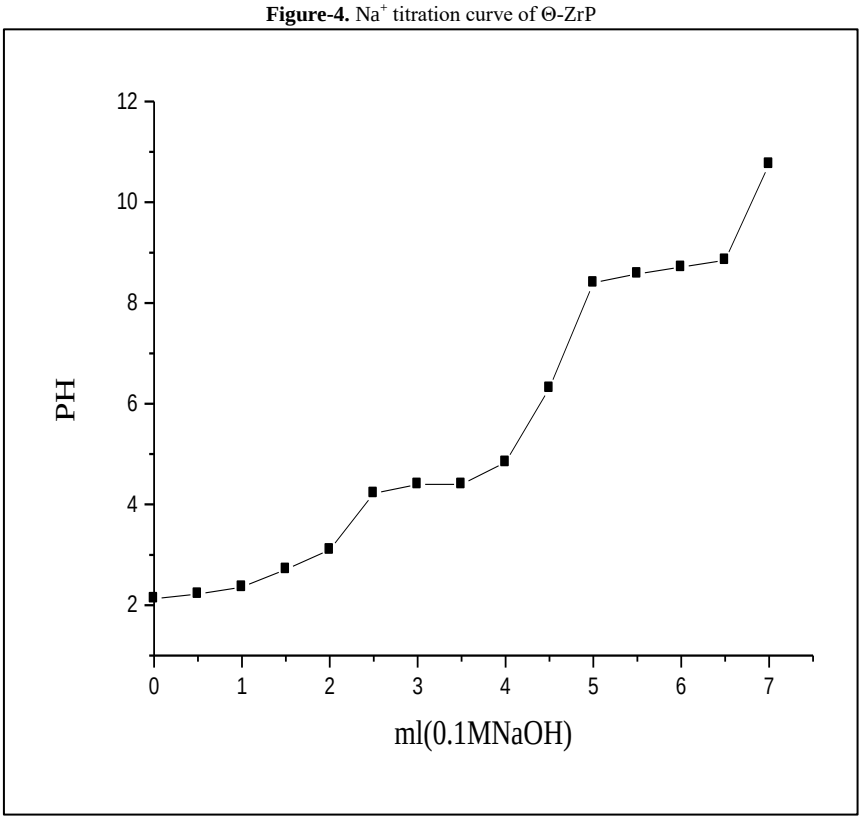

Crystalline cerium phosphate, $Ce(HPO_4)_2.1.33H_2O$(CePc), was prepared and characterized by chemical, XRD, FT-IR spectroscopy and SEM.

3.5. XRD of CePc

X-ray diffraction pattern of crystalline cerium phosphate is shown in figure 5, its interlayer distance found to be equal to 16.05Å.

Figure-5. XRD of CePc

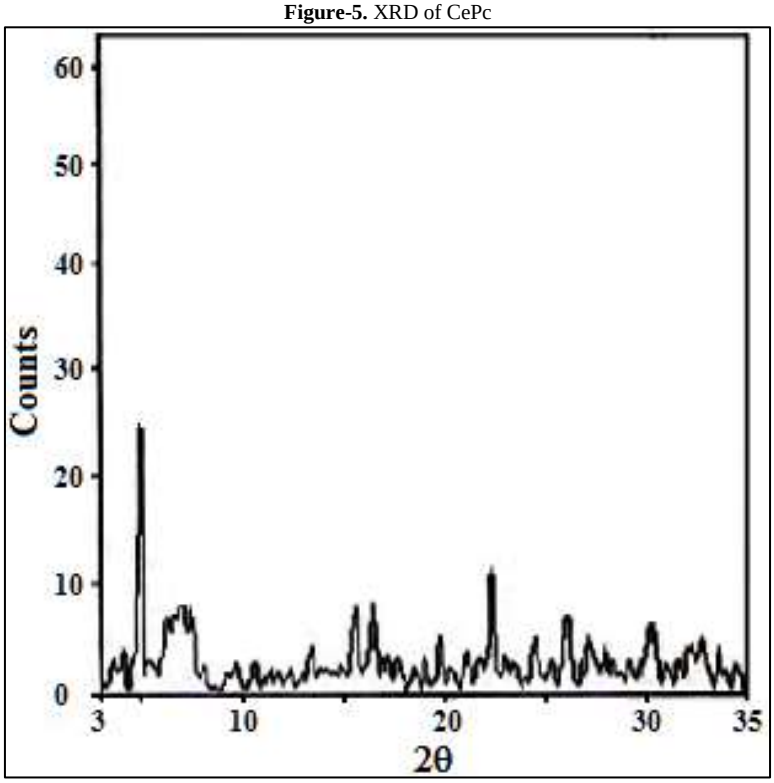

3.6. FT-IR of CePc

FT-IR spectrum of crystalline cerium phosphate is given in Figure 6. It consist of broad band centered at ~3377cm^{-1} attributed to OH groups and symmetric stretching of H_2O. Small sharp band at 1656 cm^{-1} is due to H-O-H bending. Sharp broad band centered at 1055cm^{-1} is related to the phosphate groups vibration.

Figure-6. FT-IR spectrum of CePc

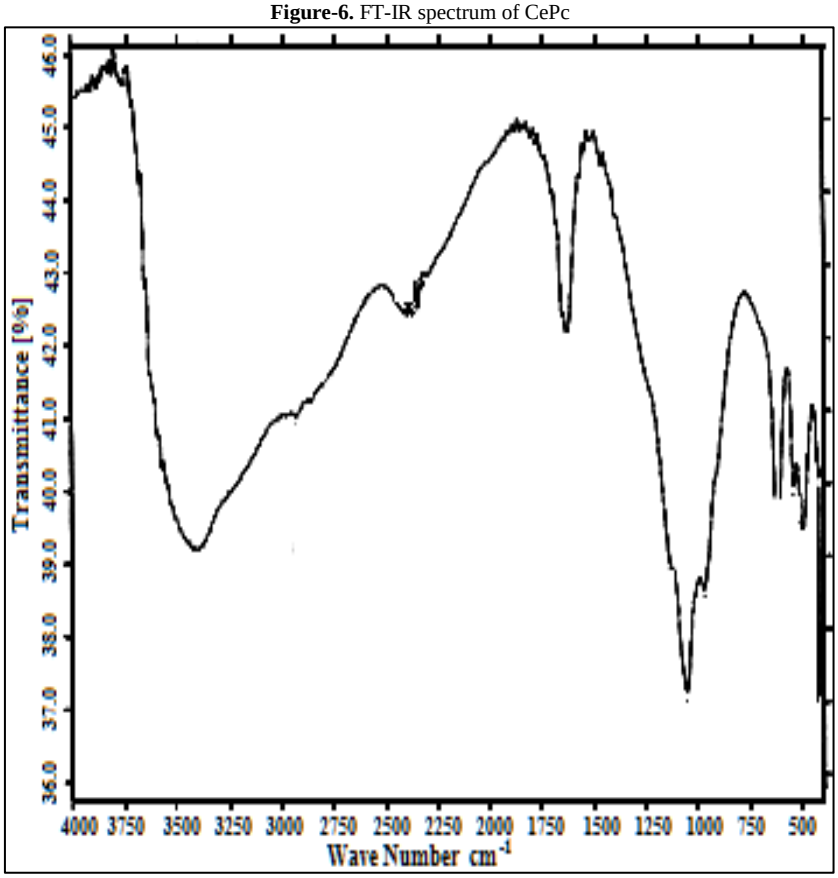

3.7. TGA of CePc

Thermal analysis of crystalline cerium phosphate is shown in Figure 7, was carried out at temperature range 25-900℃ in air atmosphere. The heating rate was 10ºC/min. the water of hydration loss occurs in the temperature range 70-250^{0}C. Above that POH groups condensation occurs. The final product was $CeO_2.P_2O_5$.

Figure-7. TGA of CePc

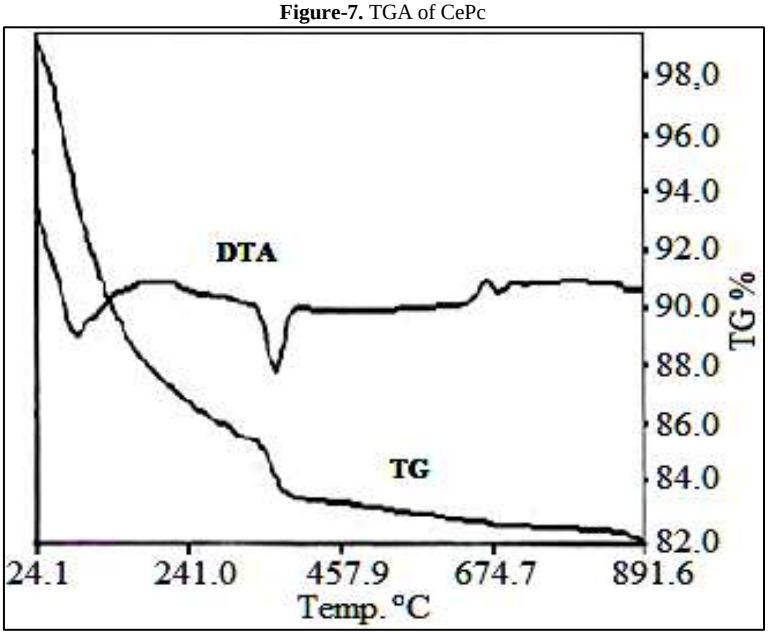

3.8. SEM of CePc

SEM morphology image of crystalline cerium phosphate is shown in Figure 8. The photograph shows its form , mainly, of compact crystallites.

Figure-8. SEM image of CePc

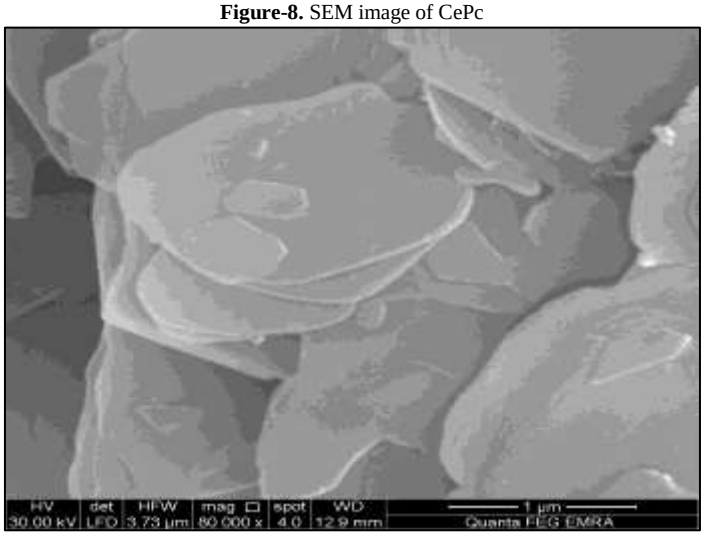

3.9. Exchange Capacity of CePc

Exchange capacity of crystalline cerium phosphate was determined by Na^+ ions titration. The titration curve is shown in Figure 9. The exchange capacity found to be equal to 2.5Meq/g.

Figure-9. Na^+ titration curve of CePc

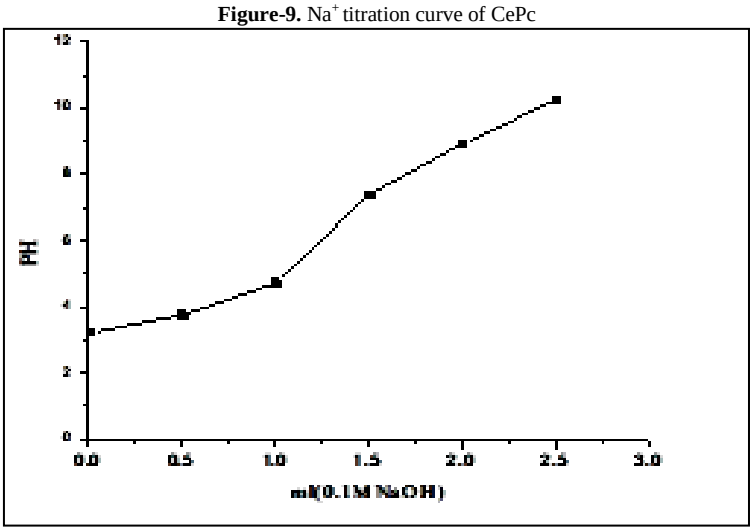

3.10. Θ-ZrP-nCePc/Polyaniline-, Polyindole-, Polycarbazole Composites

Reaction of $[\Theta\text{-}Zr(HPO_4)_2]_{0.30}[Ce(HPO_4)_2]_{0.70}\text{-}.2H_2O$ composite with the monomers, aniline, indole and carbazole, respectively led to formation of $[\Theta\text{-}Zr(HPO_4)_2]_{0.30}[Ce(HPO_4)_2]_{0.70}$ /polyaniline-, ?polyindole and / polycarbazole composites. A possible explanation is part of CePc is attacked by the monomers, respectively, converted to cerium (III) orthophosphate ($CePO_4$). During the reaction the colour gradually changes with time to bluish-green, brownish-green and green, respectively.

The resultant composites were characterized by elemental (C,H,N) analysis, FT-IR and scanning electron microscopy (SEM). From elemental (C,H,N) analysis the amount of organic materials present in Θ-ZrP-CePc/polyaniline-, polyindole-, polycarbazole composites were (23.44, 5.24, and 33.02 % in wt), respectively**.**

3.10.1. SEM of Θ-ZrP-CePc/ Polyaniline-/ Polyindole-, Polycarbazole Composites

SEM morphology images of the resultant θ-ZrP-CePc/polyaniline-, /polyindole-, and /polycarbazole composites are shown in Figures 10, 11, 12, respectively, reveal a distribution of the polymers on the inorganic matrix (Θ-ZrP-CePc).

Figure-10. SEM image of Θ-ZrP-CePc/Pani

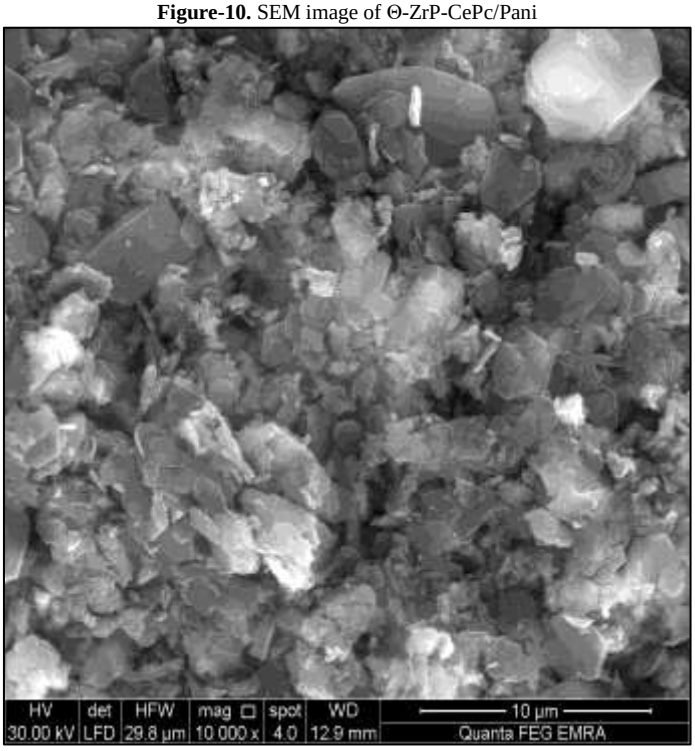

Figure-11. SEM image of Θ-ZrP-CePc/PIn

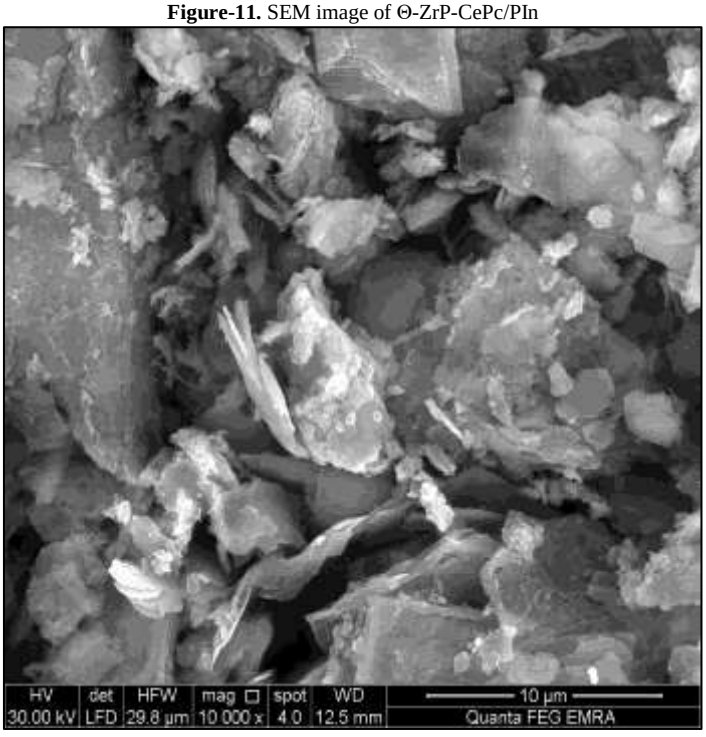

Figure-12. SEM image of Θ-ZrP-CePc/PCz.

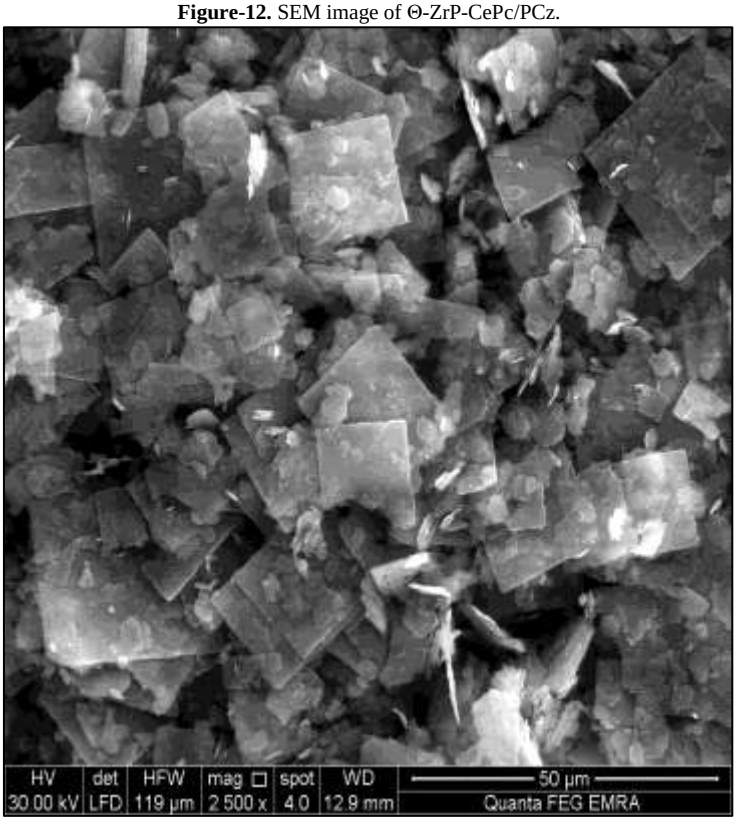

3.10.2. FT-IR Spectra of Θ-ZrP-CePc/ Polyaniline-Polyindole-, Polycarbazole composites

FT-IR spectroscopy became a key tool to investigate structure of conductive polymers and their composites.

Figures 13, 14, 15 show FT-IR spectra of Θ-ZrP-CePc/polyaniline-, /polyindole-, and /polycarbazole composites, respectively, consisting of similarity of major bands. Broad band in the range 3500-2850cm^{-1} centered ~3125cm^{-1}, is related to OH groups symmetric stretching of H_2O super imposed with the N–H stretching of aromatic amines. Medium sharp band around~ 1600cm^{-1} is related to H-O-H bending, and sharp band, centered at ~1025cm^{-1} corresponds to phosphate groups (PO_4) vibration. Bands in the range 2250-1250cm-^{1} correspond to C-H bonds and to the non-symmetric C_6 ring stretching modes. However the higher frequency vibration at ~1500cm^{-1} has a major contribution from vibration of quinoid ring of polyaniline. Other bands in the same region range are related to C-C bonds C-H (aromatic) stretching, C=C stretching. and C-N stretching of the resultant composites.

Figure-13. FT-IR spectrum of Θ-ZrP-CePc/Pani

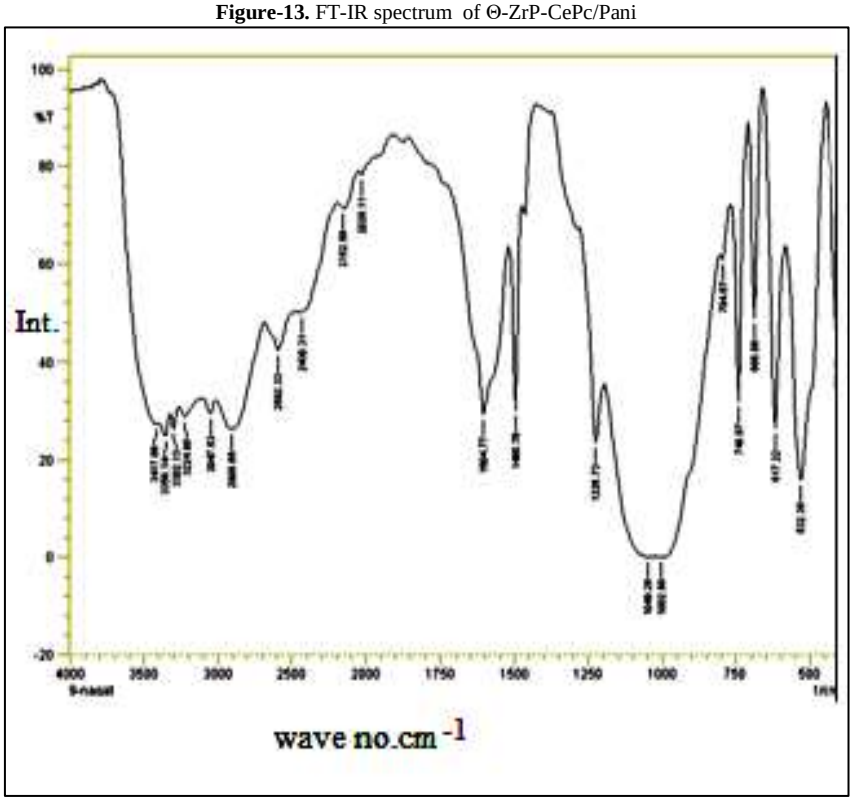

Figure-14. FT-IR spectrum of Θ-ZrP-CePc/PIn.

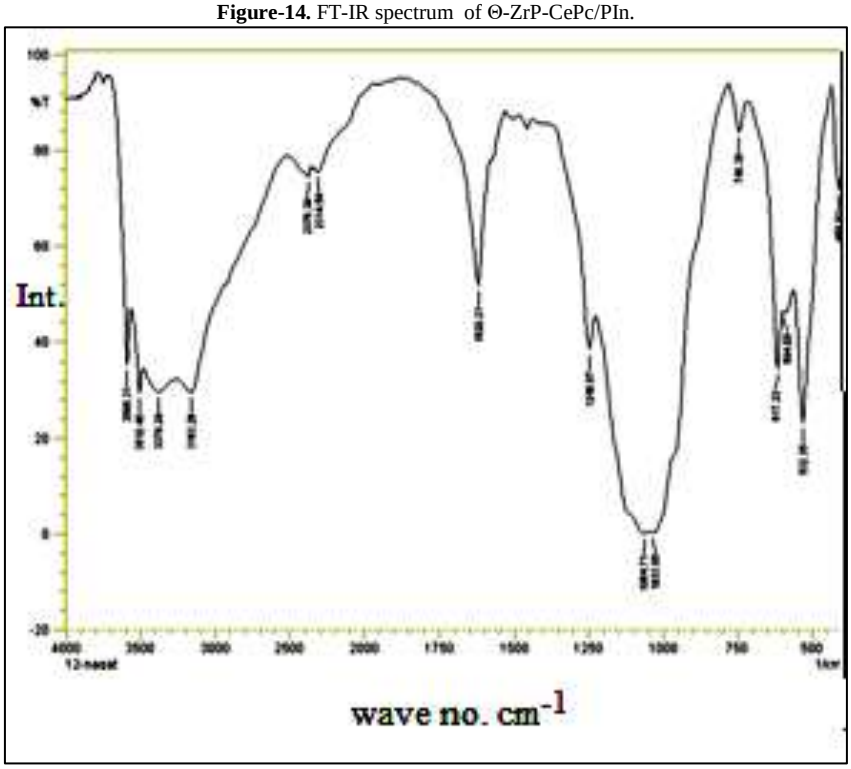

Figure-15. FT-IR spectrum of Θ-ZrP-CePc/PCz

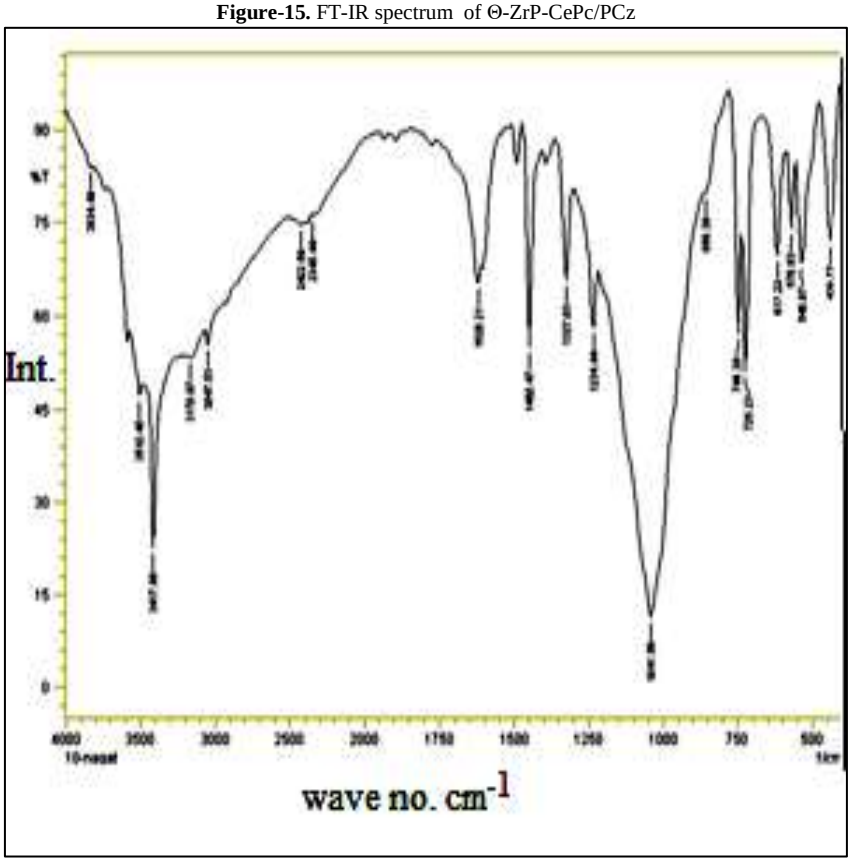

3.11. Θ-ZrP-nCePc/Polyaniline-co-Polyindole, Poly-aniline-co-Polycarbazole Composites

Reaction of $[\Theta\text{-}Zr(HPO_4)_2]_{0.30}[Ce(HPO_4)_2]_{0.70}\text{-}.2H_2O$ composite with mixtures of aniline : indole , aniline : carbazole (1:1 molar ratio), respectively, led to formation of $[\Theta\text{-}Zr(HPO_4)_2]_{0.30}$ $[Ce(HPO_4)_2]_{0.70}$ / polyaniline-co-polyindole and polyaniline-co-polycarbazole composites, respectively. A possible explanation is part of CePc is attacked by the co-monomers, respectively, converted to cerium (III) orthophosphate ($CePO_4$). During the reaction the colour gradually changes with time to brownish- green and green, respectively.

The resultant materials were characterized by elemental (C,H,N) analysis, FT-IR spectroscopy, and scanning electron microscopy (SEM). From elemental (C,H,N) analysis the amount of organic materials present in Θ-ZrP-CePc/ polyaniline-co-polyindole and polyaniline-co-polycarbazole composites were (Pani 5.92, PIn 7.48 % in wt) and (Pani 1.42, PCz 2.48 % in wt), respectively.

3.11.1. SEM Images of Θ-ZrP-CePc/Polyaniline-co-Polyindole-, Polyaniline-co-Polycarbazole Composites

SEM morphology images of Θ-ZrP-CePc / polyaniline-co-polyindole and polyaniline-co-polycarbazole composites are shown in Figures 16, 17, respectively, reveal a distribution of the copolymer on the inorganic matrix (Θ-ZrP-CePc).

Figure-16. SEM image of Θ-ZrP-CePc/Pani-co-PIn

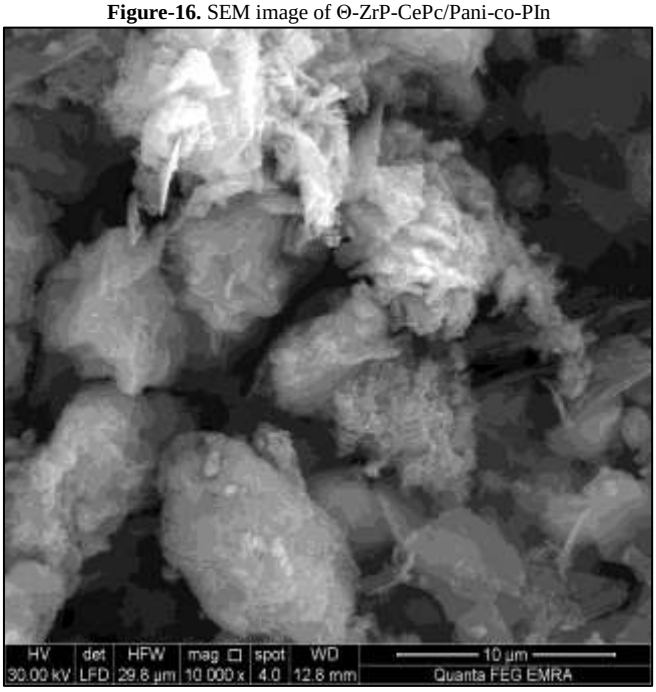

Figure-17. SEM image of Θ-ZrP-CePc/Pani-co-PCz

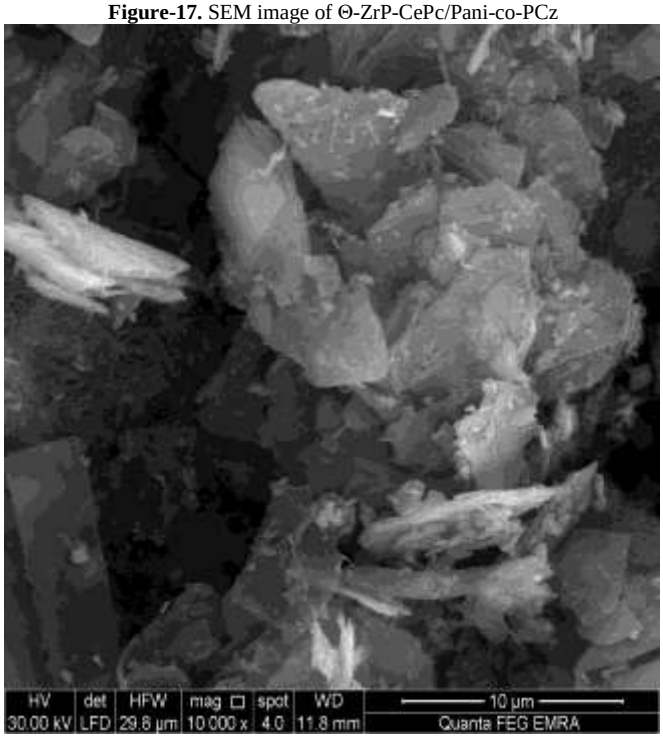

3.11.2. FT-IR Spectra of $[\Theta\text{-}Zr(HPO_4)_2]_{0.30}[Ce\text{-}(HPO_4)_2]_{0.70}$ / Polyaniline-co-Polyindole Composite

Figure 18 shows FT-IR spectrum of $[\Theta\text{-}Zr(HPO_4)_2]_{0.30}[Ce(HPO_4)_2]_{0.70}$/ polyaniline-co-polyindole composite. Consists of broad band in the range 3600-2800cm^{-1} centered ~3250cm^{-1} is due to OH groups symmetric stretching of H_2O super imposed with the N–H stretching of aromatic amines . Medium sharp band around ~1605cm^{-1} is related to H-O-H bending, sharp band ,centered at 1056cm^{-1} corresponds to phosphate groups (PO_4) vibration. Small band at ~2500cm^{-1} corresponds to C-H bonds. However the higher frequency vibration at ~1495cm^{-1} has a major contribution from vibration of quinoid ring, of polyaniline . Other bands in the range ~2400-1200cm^{-1} correspond to the non-symmetric C_6 ring stretching modes , C-C bonds, C-H (aromatic) stretching, C=C stretching and C-N stretching.

Figure-18. FT-IR spectrum of Θ-ZrP-CePc/Pani-PIn

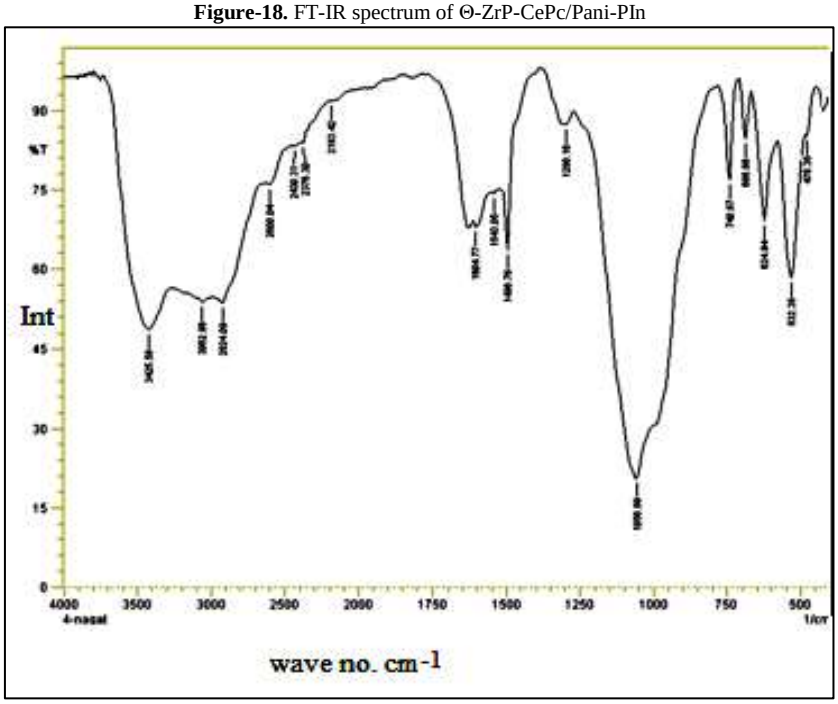

3.11.3. FT-IR Spectra of $[\Theta\text{-}Zr(HPO_4)_2]_{0.30}$- $[Ce(HPO_4)_2]_{0.70}$/Polyaniline-co-Polycarbazole Composite

Figure 19 shows FT-IR spectrum of $[\Theta\text{-}Zr(HPO_4)_2]_{0.30}[Ce(HPO_4)_2]_{0.70}$/ polyaniline-co- polycarbazole composite. Consists of broad band in the range 3600-3000cm^{-1} centered ~3250cm^{-1} is due to OH groups symmetric stretching of H_2O super imposed with the N–H stretching of aromatic amines . Medium sharp band around ~1605cm^{-1} is related to H-O-H bending, sharp band ,centered at 975cm^{-1} corresponds to phosphate groups(PO_4) vibration. Small band at ~2150cm^{-1} corresponds to C-H bonds. Other bands in the range ~1500 -1150cm^{-1} correspond to the non-symmetric C_6 ring stretching modes, C-C bonds, C-H (aromatic) stretching, C=C and stretching. C-N stretching.

Figure-19. FT-IR spectrum of Θ-ZrP-CePc/Pani-PCz.

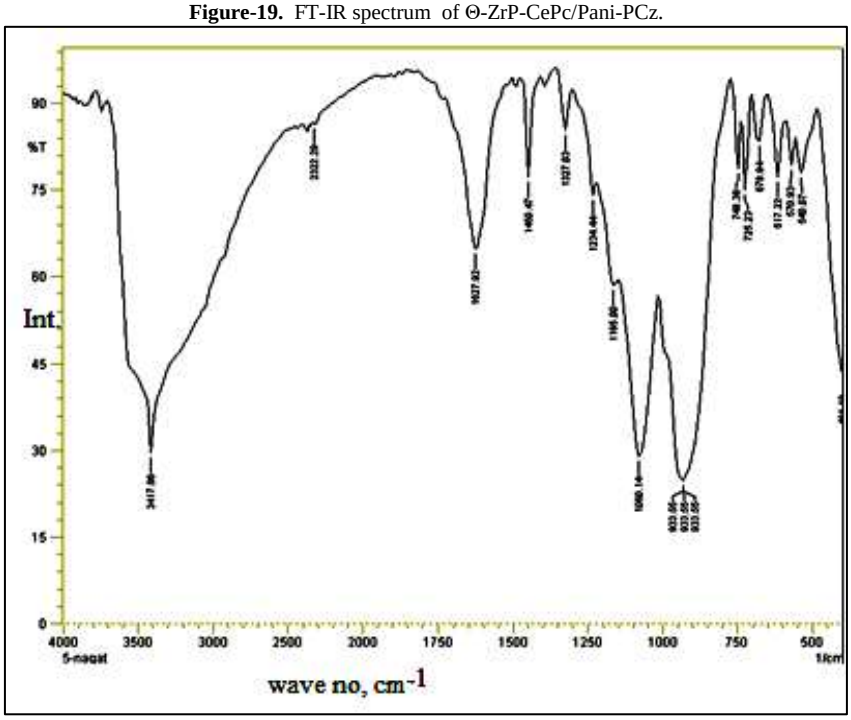

4. Conclusions

Θ-Type zirconium phosphate, $\Theta\text{-}Zr(HPO_4)_2\text{-}1.77H_2O$ (Θ-ZrP), crystalline cerium phosphate , $Ce(HPO_4)_2.1.33H_2O$(CePc), and $[\Theta\text{-}Zr(HPO_4)_2]_{0.30}[Ce\text{-}(HPO_4)_2]_{0.70}.2H_2O$ composites were prepared and characterized by chemical, XRD, TGA, FT-IR and SEM. $[\Theta\text{-}Zr(HPO_4)_2]_{0.30}[Ce(HPO_4)_2]_{0.70}$/ polyaniline, polyindole, polycarbazole, polyaniline-co-polyindole and polyaniline-co-polycarbazole composites were prepared via in-situ chemical oxidation of the monomers aniline, indole, carbazole, respectively, and their co-monomer, respectively,

that was promoted by the reduction of part of Ce(IV) ions present in the inorganic matrix. A possible explanation is part of CePc is attacked by the monomers, and the co-monomers, respectively, converted to cerium (III) orthophosphate ($CePO_4$). The resultant composites were characterized by elemental (C,H,N,) analysis, FT-IR and SEM. The formulation of the resultant novel conducting polymers and copolymers composites was supported by elemental (C,H,N) analysis, FT-IR spectra ,SEM and by colour changes. We suggest self doping occurred on polymerization, which is due to labile proton (H^+) present in (POH) groups of Θ-ZrP/CeP_c composite. These composites can be considered as novel conducting inorganic-organic composites, ion exchangers, solid acid catalysts and sensors.

Acknowledgements

To Department of Chemistry, Faculty of Science, University of Tripoli. Tripoli, Libya, for supporting this research.

References

[1] Nilchi, A., Maragheh, M. G., and Khanchi, A., 2004. "Synthesis and ion-exchange properties of crystalline titanium and zirconium phosphates." *Journal of Radioanal. and Nucl. Chem.*, vol. 261, pp. 393-400.

[2] Cheng, Y., Dong, X., Wang, T., Jaenicke, S., and Chuah, G. K., 2018. "Mechanochemistry-based synthesis of highly crystalline γ-zirconium phosphate for selective ion exchange." *Inorg. Chem.*, vol. 57, pp. 4370-4378.

[3] Shakshooki, S. K., Rhuma, A. M., and El-Akari, F. A., 2011. "Inclusion of amino acids L-alanine, L-arginine, L-serine, L- lysine, L-aspargine and proline." *J. Faulty of Edu.,Tr. Lib.*, vol. 7, pp. 1-11.

[4] Glez, J. G., Trobajo, C., Khainakov, S. A., and Amghouz, Z., 2017. "α-Titanium phosphate intercalated with propylamine: An alternative pathway for efficient europium(III) uptake into layered tetravalent metal phosphates." *Arab. J. of Chem.*, vol. 10, pp. 885-894.

[5] Cruz, E., Broker, E. J., and Mosby, B. M., 2020. "Combination of intercalation and surface modification in layered zirconium phosphates: investigation of surface stability and reactivity." *Dalton Trans.*, vol. 49, pp. 3841-3848.

[6] COnstantino, V. R. L., Barbarosa, A. S., Bizeto, M. A., and Dias, P. M., 2000. "Intercalation compounds involving inorganic layered structures." *An. Acad. Bras. Ciênc.*, vol. 72, pp. 1678-2690.

[7] La-Ginestra, A., Patrono, P., Beradell, M. L., Golli, P., Ferragina, C., and Whittaker, D., 2007. *J. Mol. Cat.*, vol. 152, pp. 187-192.

[8] Thakar, R. and Chudasama, U., 2009. "Synthesis, characterization and proton transport of crystalline zirconium titanium phosphates." *J. of Sci. and Ind. Res.*, vol. 68, pp. 312-318.

[9] Alberti, G., Cherubini, F., and Palombari, R., 1996. "Preparation, proton transport and use in gas sensors of thin film zirconium phosphate with γ-layered structure." *Sensors and Actuators*, vol. 1-2, pp. 179-183.

[10] Clearfeild, A., 1988. "Role of ion exchange in solid state Chemistry." *Chem. Review.*, vol. 88, pp. 125-148.

[11] Shakshooki, S. K., Azzabi, O. H., Khalil, S., Kowalczyk, J., and Naqvi, N., 1988. "Crystalline mixed hafnium-titanium phosphates." *Reactive Polymers*, vol. 7, pp. 191-196.

[12] Clearfield, A., 1993. "Ion exchange and adsorption in layered phosphates." *Mater. Chem. and Phys.*, vol. 35, pp. 257-263.

[13] Alberti, G., Bernasconi, M. G., Costantino, U., and Gill, G. S., 1977. "Ion exchange of trivalent cations on zirconium phosphate with large interlayer distance." *J. Chromatog.*, vol. 132, pp. 177-181.

[14] Khan, A. A., Paquiza, L., and Khan, A., 2010. "An advanced nano-composite cation-exchanger polypyrrole zirconium phosphate as a Th(IV) selective potentiometric sensor." *J. of Mater. Sci.*, vol. 45, pp. 3610-3625.

[15] Sun, L., Boo, W., Sun, D., Clearfeild, A., and Sue, H. J., 2007. "Preparation of exfoliated epoxy/α-zirconium phosphate containing high aspect ratio nanoplatets." *Chem. Mater.*, pp. 1749-1754.

[16] Feng, Y., He, W., Zhang, X., Jia, X., and Zhao, H., 2007. "The preparation of nanoparticles zirconium phosphate." *Mater. Letters*, vol. 61, pp. 3258-3261.

[17] Miguel, A., Salvadó, P. P., Camino, T., and José García, R., 2007. "Crystal structure of a cerium(IV)bis(phosphate) derivative." *J. Am. Chem. Soc.*, vol. 129, pp. 10970-10971.

[18] Tushato, M., Danjo, M., Baba, Y., Murakom, M., and Nana, H., 1997. "Preparation and chemical properties of a novel layered cerium(iv) phosphate." *Bulletin of Chem. Soc Jap.*, vol. 70, p. 143.

[19] Salvado, M. A., Pertierra, P., Tropajo, C., and Garcia, G. R., 2007. "Crystal structure of cerium(iv) bis(hydrogen phosphate) derivative." *J. Am. Chem. Soc.*, vol. 129, p. 1097.

[20] Parangi, T., Wani, P., and Chudasama, U., 2012. "Synthesis, characterization and application of cerium phosphate." *Desalination and Water Treatment*, vol. 38, p. 126.

[21] Romano, R. and Alves, O. S., 2005. "Fibrous cerium(iv) phosphate host of weak and strong Lewis bases, Inclus." *Phenom. and Macrocyclic*, vol. 51, p. 211.

[22] Casciola, M., Costantino, U., and D´amico, S., 1988. "Ac Conductivity of cerium (iv) phosphate in hydrogen form." *Solid State Ionics*, vol. 28, p. 617.

[23] MacDiarmid, A. G., 2001. "A novel role for organic polymers." *Angewandte Chemie International Edition*, vol. 40, p. 2581.

[24] Bakhashi, A. K. and Bhallal, C., 2004. "Electrically conducting polymers; materials of twenty first century." *J. of Sci. and Ind.Res.*, vol. 63, pp. 715-728.

[25] Heeger, A., 2001. "Semiconducting and metallic polymers: The fourth generation of polymeric materials." *Reviews of Modern Phys.*, vol. 73, p. 681.
[26] Lange, U., Roznyatovskaya, N. V., and Mirsky, V. M., 2008. "Conducting polymers in chemical sensors and arrays." *Analytica Chimica Acta*, vol. 614, pp. 1-26.
[27] Kucheldorf, H. R., Luken, O., and Swift, G., 2010. *Hand book of polymer synthesis*. 2nd ed. CRC Press.
[28] Bhadra, J., Alkareem, A., and Al-Thani, 2020. "A review of advances in the preparation and application of polyaniline based thermoset blends and composites." *J. of Polym. Res.*, vol. 27, p. 122.
[29] Sapurina, I. Y. and Shishov, M. A., 2012. *New polymers for special applications*. Polymer Physics, Gomes,A.S. (ed).
[30] Isah, S., 2018. "Advanced materials for energy storage devices." *Review article Asian J. of Nanosci. and Mater.*, vol. 1, pp. 87-100.
[31] Street, G. B. and Clarke, T. C., 1981. "Conducting polymers: A review of recent work IBM." *J. Res. Dev.*, vol. 25, pp. 51-57.
[32] Skotheim, T. J. and Reynolds, J. R., 1997. *Hand-book of conducting polymers*. 3rd ed. Boca Raton, USA: CRC Press.
[33] Nalwa, H. S., 1997. *Handbook of organic conductive molecules and polymers* vol. 2. Chichester, UK: John Wiley.
[34] Freund, M. S. and Deore, B. A., 2007. *Self doped conducting polymers*. John Wiley and Sons.
[35] Lange, U., Roznyatovskaya, U., Mirskyand, N. V., and Vladimir, M. M., 2008. "Conducting polymers in chemical sensors and arrays." *Analytica Chimica Acta*, vol. 614, pp. 1-26.
[36] Banerjee, S. and Tayagi, A. K., 2012. "Functional materials: Preparation." *Processing and Applications, Elsevier*,
[37] Cai, Z., Grang, M., and Tang, Z., 2004. "Novel battery using conducting polymers: and polyaniline." *J. of Maer. Sci.*, vol. 39, p. 4001.
[38] Ćirić-Marjanović, G., 2010. *Polyaniline nanostructures, in nanostructured conductive polymers*. John Wiley and Sons, Ltd: Eftekhari, A. (ed).
[39] Vernitskaya, T. V., Tat'yana, V. V., and Efimov, 1997. "Polypyrrole: a conducting polymer; its synthesis, properties and applications." *Russ. Chem. Rev.*, vol. 66, p. 443.
[40] Fajan, A. and Been, B., 2013. "Structural and optical properties of polyindole manganese oxide nanocomposite." *Indian J. of Adv. in Chem. Sci.*, vol. 2, pp. 95-96.
[41] Wang, C., Yu, H. C., and Chen, K., 2018. "Cliplike polyaniline nanofiber synthesized by an in-situ chemical oxidative polymerization and its strong electro rheological behavior." *Synthetic Metals*, vol. 239, pp. 1-12.
[42] Macdiarmid, A. G. and Epstein, A. J., 1993. "Conducting polymers: past, present and future." *Springer*, vol. 328, pp. 133-144.
[43] Anderson, T. and Roth, S., 1994. "Conducting polymers: Electrical transport and current applications." *Brazilian J. of Physics*, vol. 24, p. 746.
[44] Mashat, L. A., Tran, H. D., Wlodarski, W., Kaner, R. B., and Zadeh, K. K., 2008. "Conductometric hydrogen gas sensors based on polypyrrole nanofibers." *IEEE Sensors*, vol. 8, pp. 365-370.
[45] Sharmaa, A. K., Sharmab, Y., and Gandhia, S., 2012. ",Characterization of Poly (aniline-co-pyrrole)/carbon nanotube composites prepared via in-situ chemical, mechanical mixing and microwave assisted methods of polymerization." *J.Adv. in Poly. Sci. and Tech.*, vol. 2, pp. 39-42.
[46] Chandrasekhar, P., 2020. *Conducting polymers, fundamentals and applications*. Springer Nature Switzerland.
[47] Ramanavičienė, A. and Malinauskas, A., 2008. "Review article: Electrochemical sensors based on conducting polymer polypyrrole." *Sensors and Actuators, B: Chemical*, vol. 128, pp. 366-373.
[48] Waghuley, S. A., Yenorkar, S. M., Yawale, S. S., and Yawale, S. P., 2006. "Application of chemically synthesized conducting polymer-polypyrrole as a carbon dioxide gas sensor." *Electrochimica Acta*, vol. 51, pp. 6025-6037.
[49] Xiaodong, H., Yue, L., Yang, L., Xu, W., Jiawei, F., and Xuelei, W., 2020. "Review: Application progress of polyaniline, polypyrrole and polythiophene in lithium-sulfur batteries." *Polymers*, vol. 12, p. 331.
[50] Alan, M. G., 1997. "Polyaniline and polypyrrole: Where are we headed." *Synthetic Metals*, vol. 84, p. 27.
[51] Dimitra, S. and P., P., 2017. "Deshpande Conducting polyaniline nanocomposite-based paints for corrosion protection of steel." *Chemical Papers*, vol. 71, pp. 459-487.
[52] Vecino, M., González, I., Muñoz, M. E., Santamaría, A., Ochoteco, E., and Pomposo, J. A., 2004. "Synthesis of polyaniline and application in the design of formulations of conductive paints." *Polym. Adv. Tech.*, vol. 15, pp. 560-563.
[53] Ebrahim, M., Abd-ElLatif, M. M., Gad, A. M., and Soliman, M. M., 2010. "Cyclic voltammetry and impedance studies of electrodeposited polypyrrole nanoparticles doped with 2-acrylamido-2-methyl-1 propanesulfonic acid sodium salt." *Thin Solid Films*, vol. 518, pp. 4100-4105.
[54] Lee, J. K., Jeong, H., Lassarote, R., Lavall, R. L., Busnaina, A., Younglae, K., Jung, Y. J., and Lee, H. Y., 2017. "Polypyrrole films with micro/nanosphere shapes for electrodes of high performance supercapacitors." *ACS Appl. Mater. Interfaces*, vol. 9, pp. 33203-33211.

[55] Chitte, H. K., Shinde, G. N., Bhat, N. V., and Walunj, V. E., 2011. "Synthesis of polypyrrole using ferric chloride (fecl3) as oxidant together with some dopants for use in gas sensors." *Journal of Sensor Tech.,* vol. 1, pp. 2161-1238.

[56] Hai1, V. V. T., Hang, T., Thi Xuan, H. T. T., Thi, N. P., Thom, N. T., Nguyen Thi, N., Didier, D. T., and Thi Mai, D. T., 2018. "Synthesis of silica/polypyrrole nanocomposites and applica-tion in corrosion protection of carbon steel." *J. of NanoSc. and Nanotech.,* vol. 18, pp. 4189-41957.

[57] Ermişn, N. and Tınkılıç, N., 2018. "Preparation of molecularly imprinted polypyrrole modified gold electrode for determination of tyrosine in biological samples." *Int. J. Electrochem. Sci.,* vol. 13, pp. 2286-2298.

[58] Billand, B., Maarouf, E., and Hamecant, E., 1994. "An investigation of electrochemically and chemically polymerized polyindole." *Mater. Rech. Bull.,* vol. 29, p. 1239.

[59] Kucheldorf, H. R., Luken, O., and Swift, G., 2010. *Handbook of polymer synthesis*. CRC Press.

[60] Cai, Z., Grang, M., and Tang, Z., 2004. "Novel battery using conducting polymers indole and polyaniline." *J. of Mater. Sci.,* vol. 39, pp. 4001-4003.

[61] Zhijiang, C. and Guang, Y., 2010. "Synthesis polyindole and its evaluation for li-ion battery applications." *Synth. Met.,* vol. 160, pp. 1902-1905.

[62] Morin, J. F. and Leclerc, M., 2001. "Syntheses of Conjugated Polymers Derived From N-alkyl-2,7-carbazoles." *Macromolecules,* vol. 34, pp. 4680-4682.

[63] Raj, V., Madheswari, D., and Mubarak Ali, M., 2013. "Chemical formation, characterization and properties of polycarbazole." *J. Appl. Polym. Sci.,* vol. 111, pp. 147-154.

[64] Kayan, D. B. and Polat, V., 2017. "Improvement of electrochemical and structural properties of polycarbazole by simultaneous electro-deposition of chitosan." *Turk. J. Chem.,* vol. 41, pp. 233-242.

[65] Shakshooki, S. K., Elakari, F. A., and Alahemmer, A. A., 2020. "Glassy-, α-zirconium-tin phosphates / fibrous cerium(iv) Phosphate-nanocomposite membranes self supported aniline, its co-pyrrole and co-indole polymerization agent." In *4th international conference Theories and Application Basic and Biosciences, J. Faculty of Science University of Misurata.* pp. 335-354.

[66] Shakshoooki, S. K., El-Akari, F. A., and Aisha, S. M., 2021. "Pellicular α-zirconium phosphate phosphite-fibrous cerium phosphate/ polybenzimidazole Its -co-polyaniline/ -co-polypyrrole, and co-polyindole nanocomposite membrane, Extended Abst." In *International Conference on Applied Chemistry July 01-03, 2021 Munich, Germany.*

[67] Shakshooki, S. K., Abuain, M. A., and Amani, E.-A. M., 2015. "Nano fibrous cerium(IV) hydrogen phosphate membrane elf -Supported aniline polymerization agent." *Amer. J. of Chem.,* vol. 5, pp. 67-74.